Transport in Porous Media (2021) 137:613–627
https://doi.org/10.1007/s11242-021-01579-1

Permeability and the Ergun Equation as a Basis for Permeability Measurements of Metallic Foams and Wire Meshes

C. Celebican[2] · S. Tanefo[2] · F. Durst[1] · C. Reichel[2]

Received: 19 October 2020 / Accepted: 12 March 2021 / Published online: 5 April 2021

Abstract
This paper concerns a method and a test set-up to measure the permeability of plates of metal foams and sets of wire meshes used to control flows in fluid filters and other flow systems designed to yield constant velocity distributions over large cross sections of flows. The method is based on permeability considerations using the Ergun equation to describe the pressure losses of packages of mono-dispersed spheres. One correlation is suggested for the permeability k over the entire range of mean velocities U_0. A suitable measuring set-up was designed, built and used to measure the permeability of plates of metallic foams and sets of wire meshes. The specific objective of the present investigation was to provide permeability data for combined sets of wire meshes with flow properties that are mainly characterized by the wire meshes with the smallest mesh size. A method of data presentation is suggested that clearly illustrates the ranges of laminar and turbulent flows through the wire meshes. The results are compared with those for technical porous plates. The suggested presentation of the results indicates that the general features of the flows through porous plates of metal foams and wire meshes are the same.

Keywords Permeability · Permeabilities · Porous plate · Wire mesh · Porous media

1 Introduction and Objectives

Many studies have already been performed on flows through porous media. The available publications reflect the different shapes of pore geometries and different material properties employed in various applications in fields such as natural sciences, engineering and medicine. Transport equations for theoretical treatments of porous media flows exist in all of these fields (e.g. see Bear 1972; Celik et al. 2017; Fourar et al. 2004; Maier et al. 2003), but it is difficult to theoretically calculate the boundary conditions for a particular porous matrix based on the geometry of the pores—although some of

✉ C. Celebican
celebicancan@gmail.com

[1] FMP Technology GmbH, Am Weichselgarten 34, 91058 Erlangen, Germany

[2] Technische Hochschule Nürnberg, Keßlerplatz 12, 90489 Nürnberg, Germany

such attempts have been undertaken, as evident from Freund et al. (2003) and Zeiser et al. (2003). The publications show that correct flow boundary conditions are needed to solve the available transport equations. Implementing these conditions in the form of theoretical treatments of flows through porous media is time-consuming, and measurements of the flow velocity U_0 and the pressure drop or pressure gradient ($\mathrm{d}P/\mathrm{d}x$) are therefore generally used to yield $U_0 = f(\mathrm{d}P/\mathrm{d}x)$. It is then possible to derive the permeability k (e.g. see Bird et al. 1960; Fourar et al. 2004):

$$U_0 = k\frac{1}{\mu}\left(\frac{\mathrm{d}P}{\mathrm{d}x}\right) \tag{1}$$

where k is supplied by:

$$k = U_0\mu\left(\frac{\mathrm{d}x}{\mathrm{d}P}\right) \tag{2}$$

This paper is based on the Ergun equation in the form given by Bird et al. (1960):

$$\frac{P_0 - P_L}{L} = 150\frac{\mu}{\mathrm{d}_\mathrm{S}^2}\frac{(1-\varepsilon)^2}{\varepsilon^3}U_0 + 1.75\frac{\rho}{\mathrm{d}_\mathrm{S}}\frac{(1-\varepsilon)}{\varepsilon^3}U_0^2 \tag{3}$$

where P_0 is the pressure in the inlet plane of the porous medium, P_L the pressure at a distance L downstream of the inlet, μ the dynamic viscosity, U_0 the inlet mean velocity (i.e. the approach velocity of the free stream), d_S the sphere diameter forming the porous matrix and ε the porosity of the package of the spheres. Introducing Eq. 3 into Eq. 1 or 2 yields a correlation $k = f(1/U_0)$ which is derived in Sect. 2 of the paper. Using $k = f(1/U_0)$, it is shown that the flow properties in the k–$(1/U_0)$-plane can be subdivided into two regions: one in which $k = k_0$, where the flow is presumed to be laminar, and another region with $k \sim (1/U_0)$, where the flow is presumed to be turbulent. The dividing line between these two regions is derived for porous media flows described by the Ergun equation (Eq. 3).

The theoretical considerations in Sect. 2 are extended to describe a k–$(1/U_0)$-correlation that also covers the transition region between the laminar and turbulent flows. One single correlation is suggested that covers the k-behaviour over the entire range of $(1/U_0)$. Based on this finding, the authors suggest the development of a measuring method based on the Ergun equation and the application of this method to characterize the general permeability behaviour of porous media flows through plates of metallic foams and sets of wire meshes.

The employed test set-up is described in Sect. 3, and preliminary results are presented to show that the test set-up properties permit permeability measurements over four orders of magnitude of k. The actual measurements are then summarized for the porous media consisting of metallic foams with high permeabilities, followed by k-measurements for combined layers of wire meshes. All the data fit the general properties of k-values for porous media flows, as derived in Sect. 2 of this paper. Based on this finding, the authors suggest permeability measurements in the manner described in Sects. 2 and 3 and the extraction of k_0, $\left(\nu C_k\right)_{k_0}$ and n from the measured data. These three parameters are introduced in Sect. 2 for porous media flows described by the Ergun equation and for n in Sect. 5.

The authors' work described in this paper is summarized in Sect. 5 and an outlook is presented with suggestions for future investigations. Suggestions are also made as to how this work can be used to perform k-value measurements for other types of porous media flows.

2 Theoretical Considerations

In Bird et al. (1960), the following relation is given for the pressure loss (dP/dx) in porous media, with parameters corresponding to those of Eq. 3:

$$\frac{dP}{dx} = 150\frac{\mu}{d_s^2}\frac{(1-\varepsilon)^2}{\varepsilon^3}U_0 + 1.75\frac{\rho}{d_s}\frac{(1-\varepsilon)}{\varepsilon^3}U_0^2 \tag{4}$$

Equation 1 and 4 can be combined to obtain:

$$U_0\frac{\mu}{k} = 150\frac{\mu}{d_s^2}\frac{(1-\varepsilon)^2}{\varepsilon^3}U_0 + 1.75\frac{\rho}{d_s}\frac{(1-\varepsilon)}{\varepsilon^3}U_0^2 \tag{5}$$

Dividing this equation by U_0 and by μ and introducing the kinematic viscosity $\nu = \mu/\rho$ yields:

$$\frac{1}{k} = 150\frac{1}{d_s^2}\frac{(1-\varepsilon)^2}{\varepsilon^3} + 1.75\frac{1}{\nu d_s}\frac{(1-\varepsilon)}{\varepsilon^3}U_0 \tag{6}$$

And, if rewritten, results in the following form of the equation for $(1/k)$:

$$\frac{1}{k} = 150\frac{1}{d_s^2}\frac{(1-\varepsilon)^2}{\varepsilon^3}\left(1 + \frac{7}{600}\frac{d_s}{\nu}\frac{U_0}{(1-\varepsilon)}\right) \tag{7}$$

Equation 6 might also be expressed in terms of the measured pressure drop:

$$\frac{1}{k} = \underbrace{150\frac{1}{d_s^2}\frac{(1-\varepsilon)^2}{\varepsilon^3}}_{(1/k_0)}\left(1 + \frac{7}{600}\frac{d_s}{\nu^2\rho}\frac{k}{(1-\varepsilon)}\left(\frac{dP}{dx}\right)\right) \tag{8}$$

The relations of Eqs. 7 and 8 show that the results of k-measurements possess two distinct regions which exist for k-variations with pressure gradients (Eqs. 9 and 10) or with volume flow rates U_0A or mean velocities U_0:

$$k = k_0 = \frac{d_s^2}{150}\frac{\varepsilon^3}{(1-\varepsilon)^2} = \text{const.} \tag{9}$$

and

$$k^2 = k_0\frac{600}{7}\frac{\nu^2\rho(1-\varepsilon)}{d_s}\left(\frac{dx}{dP}\right) \tag{10}$$

If we express the permeability k in terms of $(1/U_0)$ we can derive:

$$k = k_0\frac{600}{7}\frac{\nu(1-\varepsilon)}{d_s}\frac{1}{U_0} \tag{11}$$

In view of the derived Eqs. 9 and 11, it is very likely that similar relations can be derived for other porous media with different shapes of the pores and different porosities for a unified presentation. The permeability should always be expressible in forms of:

- Laminar flow region

$$k = k_0 = \text{const.} \tag{12}$$

- Turbulent flow region

$$k = k_0 \nu C_k \left(\frac{1}{U_0} \right) \tag{13}$$

Selecting for $k_0 = 10^{-8}$ (m^2) yields $\nu = 1.53 \times 10^{-5}$ (m^2/s), $d_s^2 = 150 k_0 \frac{(1-\varepsilon)^2}{\varepsilon^3}$ and, therefore, $d_S \approx 29 \times 10^{-4}$ (m) for $\varepsilon = 0.4$. Using these quantities, it is possible to calculate for $\nu = 1.53 \times 10^{-5}$ (m^2/s) from Eq. 11:

$$k = 2.71 \times 10^{-9}\,(\text{m}^3/\text{s}) \cdot \left(1/U_0\right)$$

Selecting for $k_0 = 10^{-10}$ (m^2) yields $\nu = 1.53 \times 10^{-5}$ (m^2/s), $d_S \approx 29 \times 10^{-5}$ (m), and the quantity k can therefore be expressed as:

$$k = 2.71 \times 10^{-10}\,(\text{m}^3/\text{s}) \cdot \left(1/U_0\right)$$

and so on, permitting compilation of the diagrams in Fig. 1.

A further generalization of permeability as a function of $(1/U_0)$ can be derived if we express Eq. 13 in the following form:

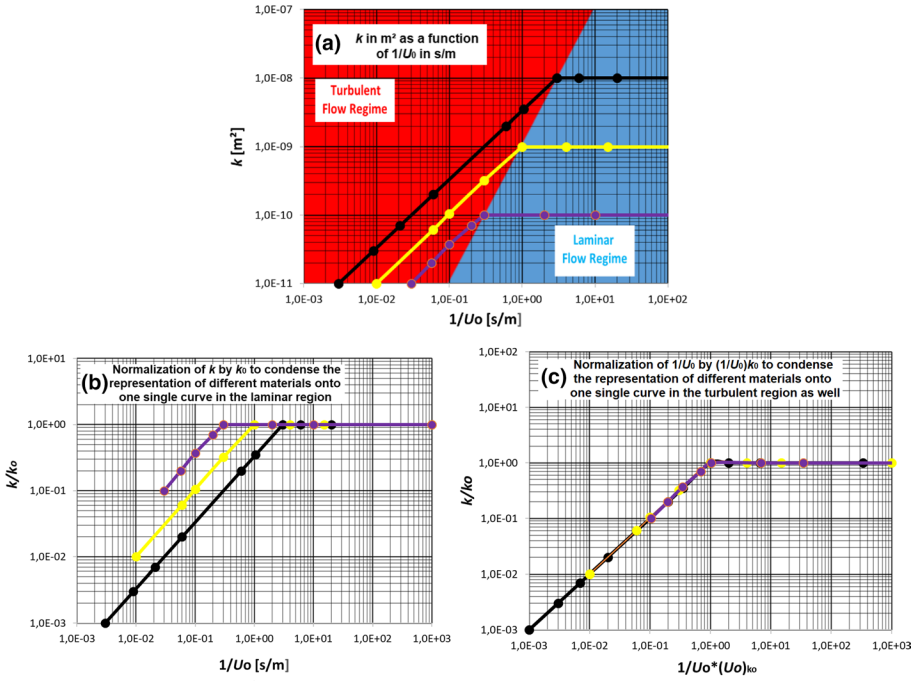

Fig. 1 Double logarithmic diagrams of permeability k as a function of $(1/U_0)$ for flows through plates of metallic foams expected from the Ergun equation

$$\frac{k}{k_0} = \nu C_k \left(\frac{1}{U_0}\right) \rightarrow \log_{10}\left(\frac{k}{k_0}\right) = \log_{10}\left(\nu C_k\right) + \log_{10}\left(\frac{1}{U_0}\right); \quad k \leq k_0 \tag{14}$$

The term $\log_{10}\left(\nu C_k\right)$ can be separated into contributions of fluid and contributions of pore size and geometry if written as:

$$log_{10}(\nu C_k) = \overbrace{log_{10}\nu}^{Influence\ of\ fluid} + \underbrace{log_{10}C_k}_{Influence\ of\ pores} \tag{15}$$

The presentation of results of k-measurements in double logarithmic diagrams, therefore provides insights into the influence of fluid and pore geometry on the permeability of porous media flows.

The presentation of k-results in Fig. 1 suggests that the behaviour of k in the laminar flow region can be fully characterized by the permeability k_0, as expressed by Eq. 12. This means that presentation of the results as $\log_{10}\left(\frac{k}{k_0}\right)$ provides a more generalized picture (see Fig. 1b). Finding the point for each set of the results where $k = k_0$ i.e. $\left(\frac{k}{k_0}\right) = 1$ yields from Eq. 14:

$$0 = \log_{10}\left(\nu C_k\right)_{k_0} + \log_{10}\left(\frac{1}{U_0}\right)_{k_0} \tag{16}$$

resulting in correlation for all permeabilities of packed beds of spheres when plotted as:

$$\log_{10}\left(\frac{k}{k_0}\right) = \log_{10}\left(\nu C_k\right) + \log_{10}\left[\left(\frac{1}{U_0}\right)\left(U_0\right)_{k_0}\right].$$

This function is presented in Fig. 1c.

Although the above relations were derived solely from the Ergun equation, the results of the derivations should also be applicable to porous media that are not made up of spherical particles. One aim of the authors investigations was to show that this is the case for porous matrices consisting of metallic foams with open pores and for sets of wire meshes. The two sets of results are presented in Sects. 3 and 4 of this paper, respectively.

The above considerations suggest that the entire permeability distribution for porous media flows can be expressed by the parameters k_0 and $\left(\nu C_k\right)_{k_0}$, yielding the following relations:

- Laminar flow:

$$k_0 = \text{const.} \tag{17}$$

- Turbulent flow:

$$\frac{k}{k_0} = \nu C_k \left(\frac{1}{U_0}\right) \tag{18}$$

or:

$$\log_{10}\left(\frac{k}{k_0}\right) = \log_{10}\left(\nu C_k\right) + \log_{10}\left(\frac{1}{U_0}\right) \tag{19}$$

3 Permeability Measurement of Metallic Foams

In recent years, metallic foams have been brought onto the market in the form of solid materials with cellular structures possessing high porosities. Porosity values of $\varepsilon = 75$–95% can be achieved, depending on the employed manufacturing method and the metal used as the base material. Due to the high porosity ε, this permits the development of lightweight structures that provide advantages for many technical applications. From a technical point of view, flow equipment that takes advantage of the special properties of metallic foams with open pores can be made available (e.g. equipment such as heat exchangers, filters, mixers, etc.). But the design of this kind of flow equipment requires information on its permeability. This information is not readily available, since manufactures of metallic foams usually only provide data on the porosity ε and on the average density ρ_{foam} as well as the metal used. The corresponding ρ_{met}-value for the latter (i.e. for ρ_{met}) can be found in the literature, so that we can write:

$$\rho_{\text{foam}} = (1-\varepsilon)\rho_{\text{met}} + \varepsilon\rho_{\text{air}} \tag{20}$$

Since $\rho_{\text{air}} \ll \rho_{\text{met}}$, the following relation can be used to calculate the porosity ε:

$$\varepsilon = 1 - \frac{\rho_{\text{foam}}}{\rho_{\text{met}}} \tag{21}$$

Knowing the porosity of a metallic foam does not enable us to design flow equipment with open pores. For this purpose, we additionally need information on the permeability k of the material in question and, as mentioned in the introduction, it is therefore necessary to conduct the corresponding measurements. To carry out such measurements, the authors designed, built and applied a suitable test set-up and used information derived in Sect. 2 to present the obtained data. One of the key aims of the authors was to show that the permeability measurements for metallic foams with open pores can be presented in the manner indicated in Fig. 1 for porous media consisting of mono dispersed spheres. For measurement purposes, a test set-up was created as shown in Fig. 2a, consisting of a large metal vessel with a volume of 120 L acting as a plenum chamber for the air flow. The top of the vessel consisted of a cover plate on which the actual test set-up was mounted. As the sketch in Fig. 2b shows, the inlet took the form of a double flange that was able to hold the round porous plate samples but also permitted the mounting of wire meshes between the flanges. Special rubber rings were used to ensure that only the "flow area" of the technical porous plates was open to the air flow. For this purpose, the authors used a pipe-and-pipe connecting system from the company "Fr. Jacob Söhne GmbH & Co. KG" (2009). The flange, pipe and rubber ring systems were easy to assemble. The border was sealed using adhesive tape to prevent air from entering from the side of the round porous plates.

The air flow for the low volume flow rates was supplied by a vacuum pump from the company "Zhejiang Wenling Hongbaoshi Vacuum Equipment Factory" (2020), and the high flow rates through the porous plates were generated by a side channel compressor from the company "FPZ" (2015). The pressure difference was measured using a manometer from the company "MRU GmbH" (2018) with a pressure range of $-7500\ \text{Pa} \le \text{d}P \le 7500\ \text{Pa}$ and

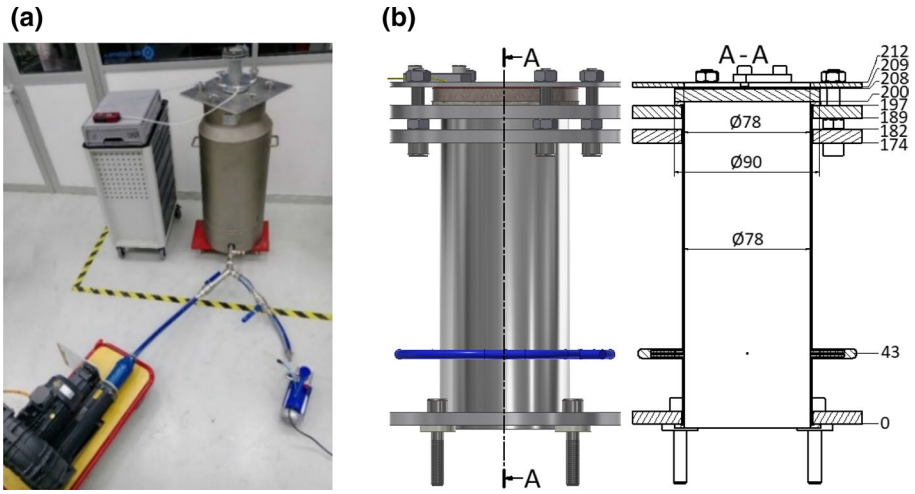

Fig. 2 Test set-up and diagram showing dimensions

a resolution of 0.1 Pa. The average velocity at the inlet of the porous plates was measured using a hot wire sensor from the company "Cambridge AccuSense Inc." (2020) with a range of 0.5 m/s $\leq U_0 \leq$ 15 m/s. These measuring ranges of the instruments ensured that it was possible to cover the laminar and turbulent regions of the flows through all the tested technical porous plates.

In a first step, the required range of average velocities and pressure losses through the porous plates were investigated using the test set-up (shown in Fig. 2a) and appropriate measuring equipment, providing the diagram shown in Fig. 3. Based on these preliminary results, the authors determined the ranges of flow rates and differential pressures required for the main experiments. Some initial tests used other pumps that did not cover the appropriate volume rates and related pressure gradients. It was therefore necessary to

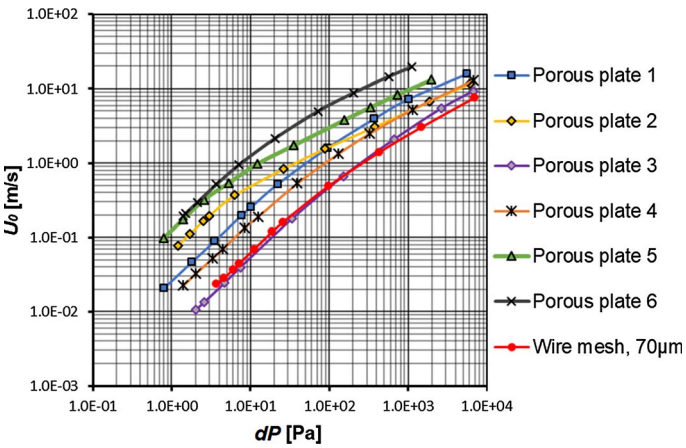

Fig. 3 Double logarithmic graph showing velocity and pressure ranges required for the permeability measurements

match the test set-up to the k-ranges for the porous plates of metallic foams that were being investigated.

The preliminary experimental test outlined above shows that the test set-up covered the expected pressure range of nearly 10^4 pressure units of pressure drop. Moreover, the measurements of the air flow rates lie within the range expected for experimental permeability measurements for metallic foam plates with a thickness of approx. 6 to 7 mm.

Details of the initial and final test set-ups are provided in Fig. 4 in the form of two photographs. Both pictures are self-explanatory so that no further descriptions of the various parts are necessary. The results provided in Fig. 3 permit the conclusion that the following two vacuum pumps should be sufficient to generate the flow for permeability measurement through technical porous plates and sets of wire meshes.

- Vacuum pump 1: oil vacuum pump; suction capacity: 127 L/min; vendor: Mucola GmbH (2020)
- Vacuum pump 2: oil-free piston vacuum pump; suction capacity: 160 L/min; vendor: Amazon.com, Inc. (2020)

The data are presented in Fig. 5a, which shows the measured k-values as a function of ($\mathrm{d}x/\mathrm{d}P$) as expressed by Eqs. 9 and 10. Figure 5b shows the equivalent presentation as

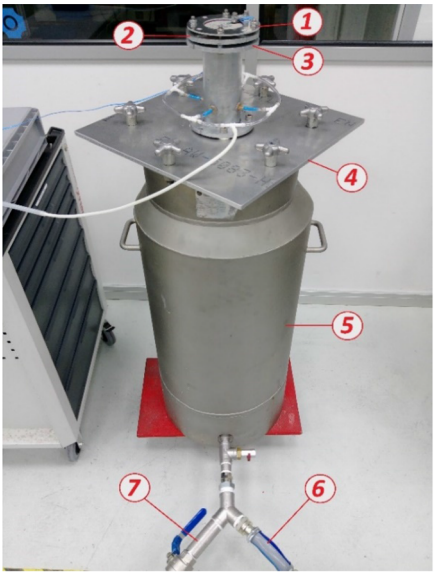

1: Flange for mounting samples, 2: Two-piece flange for central alignment of the sample, 3: Two-piece flange as counterpart of the flange above, 4: Cover plate of the plenum chamber, 5: Plenum chamber, 6: Pipe to the vacuum chamber, 7: Pipe to the side channel blower.

(a)

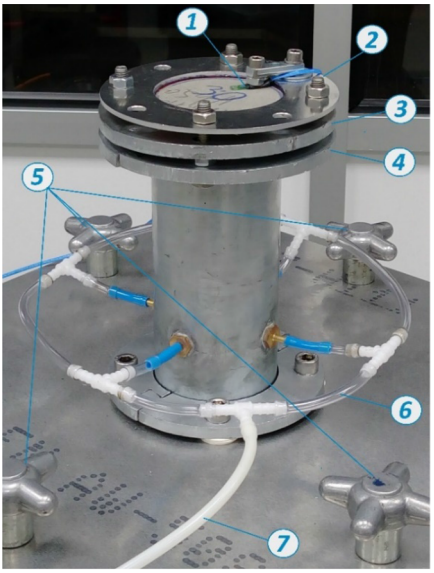

1: Hot wire sensor to measure flow velocity, 2: Flange for mounting sample, 3: Two-piece flange for central alignment of the sample, 4: Two-piece flange as counterpart of the flange above, 5: Connecting screw for the cover, 6: Hose-ring to measure pressure, 7: Connecting hose for the manometer.

(b)

Fig. 4 Details of test and measuring set-up with inlet flanges and pressure measurement ring

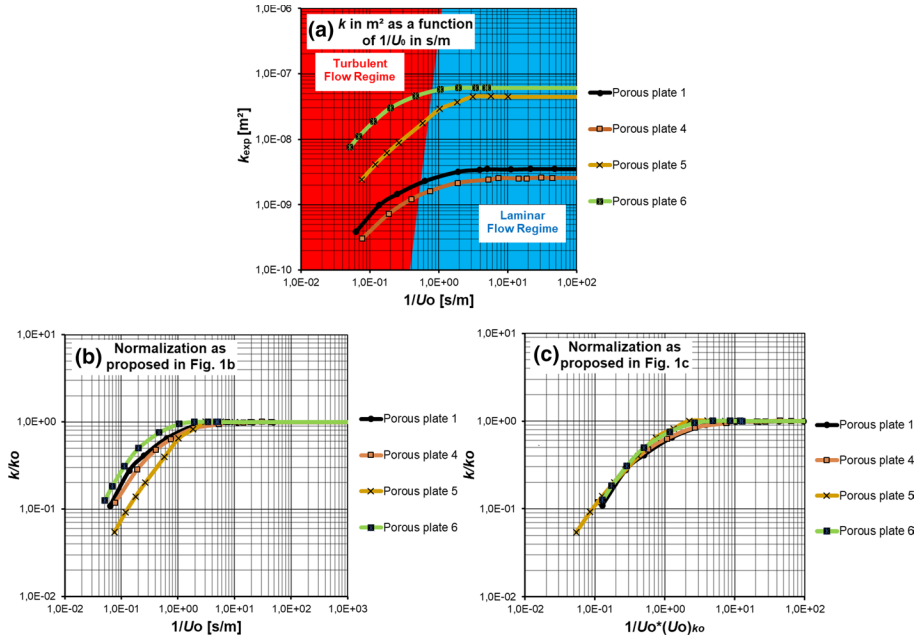

Fig. 5 Double logarithmic diagrams of results of k-measurements of metallic foams showing regions of laminar and turbulent flows in porous media

suggested by Eqs. 12 (laminar flow) and 13 (turbulent flow). Both figures show that the results derived from the Ergun equation can be similarly applied to porous media flows through metallic foams with open pores. The values of k_{exp} were calculated based on the measurement data of the velocity, the pressure loss and the thickness of the specimens using Eq. 2.

The results of the permeability measurements of metallic foams show the straight line in the turbulent flow region as predicted in Sect. 2. However, the shape of the resulting lines for the different metallic foams are flatter than those predicted by the Ergun equation.

4 Permeability Measurement of Sets of Wire Meshes

Wire meshes are metal structures made up of connected strands of metal, generally woven into a networked structure and forming square or rectangular openings between wires. These wire meshes can be manufactured using different methods and can be made out of different materials depending on the applications. There are many designs with rectangular openings ranging from simple household applications (tea strainer) and protection devices (Faraday cages), to fluid filtration systems and printing devices (screen printing) etc. For some of these applications, it is advantageous to employ sets of wire meshes consisting of wire screens of different mesh openings and different wire diameters. These types of wire meshes are shown in Fig. 6.

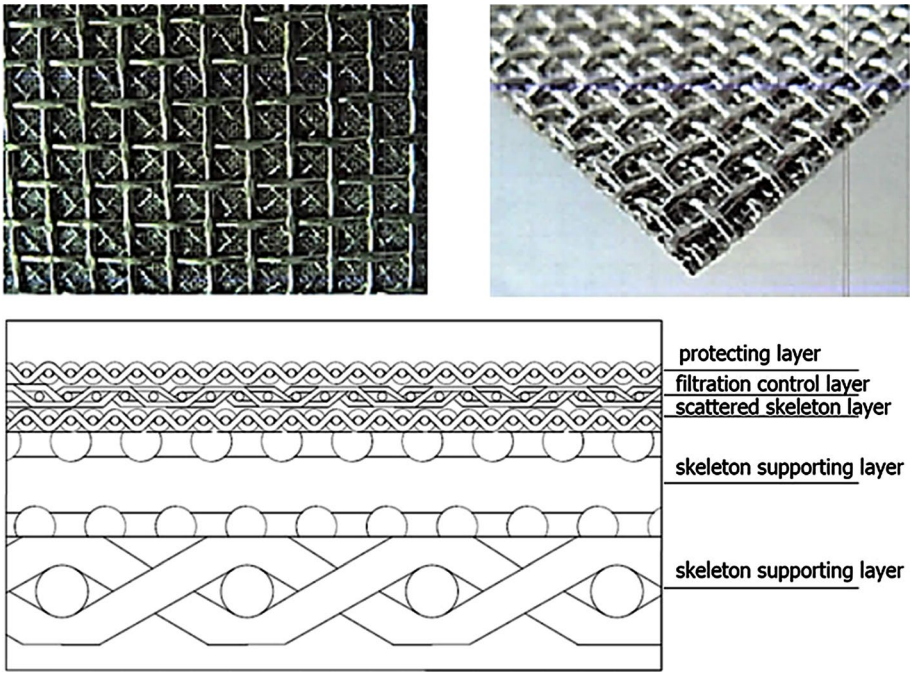

Fig. 6 Examples of sets of wire meshes: the different mesh layers can be connected by sintering or welding

Sets of wire meshes can also be used in flow equipment to ensure equalization of fluid velocities over larger flow areas—in the air dryers used in the coating industry, for example. Further applications can be found in fluid filtration systems, where the reinforcing layers ensure the mechanical strength of the wire mesh structure and the control layer supports the functional properties of the filter.

The aforementioned applications of sets of wire meshes must be based on functional layout considerations, which in turn require permeability information. This information is not readily available, and the authors therefore used the measuring equipment described in Sect. 3 to carry out U_0-(dP/dx)-measurements, using the results to derive the k-values of sets of wire meshes. These steps and the corresponding results are described on the following pages.

Before the wire mesh permeability measurements were performed, samples had to be prepared so that they were suitable for the authors' test set-up. Such a sample is shown in Fig. 7. Rubber rings were placed along the peripheries of the samples to prevent the air flow from passing sideways through the wire mesh samples during the permeability measurements.

The wire meshes used by the authors had total thicknesses of 1.7–1.9 mm. The sample holder had to be modified to permit installation of the meshes in the inlet port of the test set-up. A top flange was installed as shown in Fig. 4. With the help of this flange, the wire meshes were aligned to the next flange, and the rubber sealing ring ensured that the air flow was guided through the mounted wire meshes to yield a flow area of 4778.4 mm^2. This arrangement provided the permeability measurements listed below. The results were evaluated using the same procedure as that employed for evaluation of the k-results for the porous plates made of metallic foam.

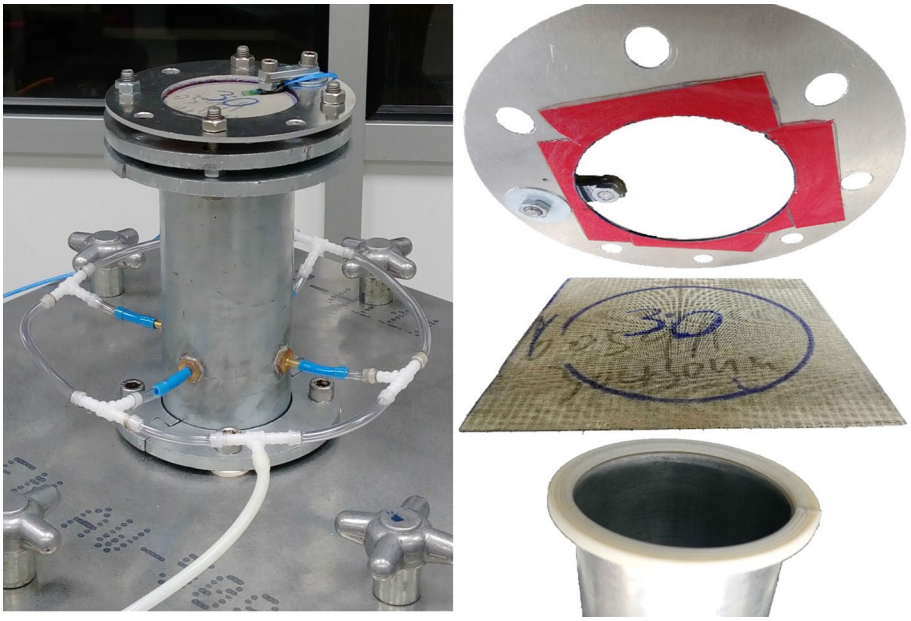

Fig. 7 Prepared wire mesh sample to investigate the permeability of sets of wire meshes

The investigated wire meshes were made up of six layers of wires each with different mesh sizes. The largest wire meshes had a mesh size of 400 μm, while the smallest mesh size was in the range from 20 to 100 μm. The smallest sizes were used to characterize each sample, as information on the sizes of all the remaining layers was not available. In other words, sets of wire meshes with the smallest mesh sizes of 20, 30, 40, 50, 60, 70, 100 μm were used by the authors to measure their permeability. These measurements supplied the results shown in Fig. 8, yielding k-distributions that show constant k-values in the laminar flow regime in the range of 10^{-11} (m^2)$\lesssim k \lesssim 10^{-9}$ (m^2). In the turbulent flow regime, the linearity of the k-variation with (dx/dp) found for technical porous plates was also found for the investigated wire meshes. The theoretically derived variation for k over (dx/dP) was found with a slope of ½, corresponding to a dependence of k on the square of the flow velocity for large U_0 or large $(\mathrm{d}P/\mathrm{d}x)^{-1}$-values of the air flow through the wire meshes.

Material properties of each respective set of wire meshes:

- Wire mesh, 20 μm: dx = 1.80 mm, ε = 0.400, ρ = 7.95 g/cm^3
- Wire mesh, 30 μm: dx = 1.70 mm, ε = 0.323, ρ = 7.95 g/cm^3
- Wire mesh, 40 μm: dx = 1.80 mm, ε = 0.358, ρ = 7.95 g/cm^3
- Wire mesh, 50 μm: dx = 1.80 mm, ε = 0.363, ρ = 7.95 g/cm^3
- Wire mesh, 60 μm: dx = 1.90 mm, ε = 0.429, ρ = 7.95 g/cm^3
- Wire mesh, 70 μm: dx = 1.80 mm, ε = 0.416, ρ = 7.95 g/cm^3
- Wire mesh, 100 μm: dx = 1.78 mm, ε = 0.344, ρ = 7.95 g/cm^3

A transitional flow region exists between the $k-(\mathrm{d}P/\mathrm{d}x)^{-1}$-regions for laminar and turbulent flows. This is similar to the flow behaviour through pipes and channels, where the flow turns from a laminar state into a turbulent state. This change in flow behaviour occurs

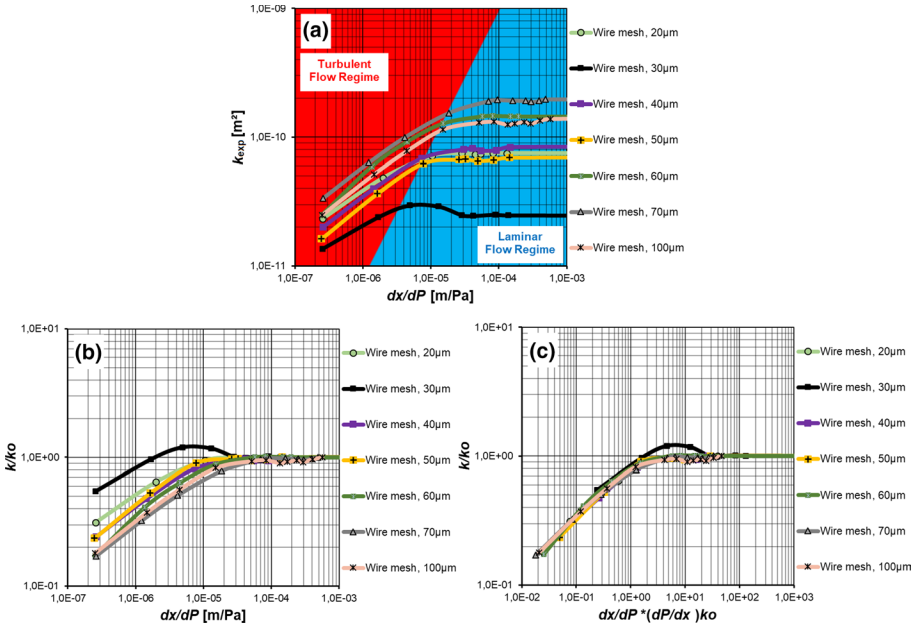

Fig. 8 Double logarithmic diagrams of permeability measurements of layers of wire meshes

intermittently in form of "puffs and slugs" [e.g. see Wygnanski and Champagne 1973 or Durst and Ünsal 2006]. This intermittent transition from laminar to turbulent also occurs in flows through porous media and is responsible for "the hump of k" for the "Wire mesh, 30 µm" shown in Fig. 8. Depending on the properties of the pore geometry, this hump may be quite pronounced as shown in Fig. 8.

In spite of these findings for the "hump-behaviour of k" in the region of laminar to turbulent transition, the general behaviour described in Sect. 2 with regard to the permeability of $k=f(\mathrm{d}x/\mathrm{d}P)$, is also confirmed for sets of wire meshes. The authors therefore suggest describing the permeability based on measurements of k_0, ν, C_k as follows:

- $k_0 = \text{const.}$ (Laminar flow) (22)

- $k = k_0(\nu C_k)\dfrac{1}{U_0}$ (Turbulent flow) (23)

The line indicating laminar-turbulent transition (i.e. between the red and blue regions in Figs. 5, 8 and 9) was determined for each sample by extrapolation of two tangents of the k-distribution, where one tangent lies in the laminar and the other in the turbulent flow regime. The graph below illustrates this using four different measurement samples as examples for drawing the dividing line between the laminar and turbulent flow regions. The slope of these generated tangents corresponds to the derivations (Eqs. 6 and 7) in Sect. 1.

The first tangent to the k-distribution is in the laminar region, while the second tangent is in the turbulent region. For each k-distribution curve, the intersection of the two tangents forms a point of laminar-turbulent transition. Finally, the straight line describing the transition region is created by connecting each of these intersections.

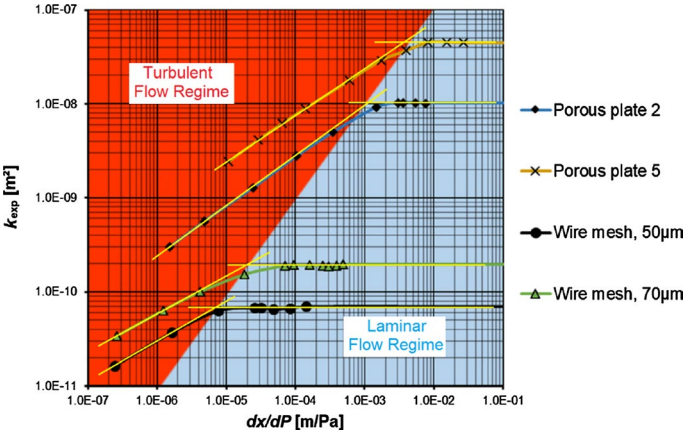

Fig. 9 Double logarithmic graph used to determine the region of laminar-turbulent transition

The combined results in Fig. 9 show that the measured permeabilities for plates of metallic foams with open pores are similar to the permeabilities for sets of wire meshes. Comparison of Figs. 1 and 9 suggests that flows through porous matrices of mono-dispersed spheres show similar permeability behaviour.

5 Conclusions, Final Remarks and Outlook

This paper describes investigations of the permeability of metallic foams with open pores and staggered layers of wire meshes. The tests were based on permeability considerations similar measurements of porous media consisting of mono-dispersed spheres. The pressure loss behaviour of the latter, as a function of the flow rate of viscous fluids, is described by the Ergun equation. This equation is used in Sect. 2 to show that the entire k-distribution conforms to the two asymptotic solutions provided by Eqs. 18 and 19. Following a suggestion of Churchill and Usage (1972), the entire k-distribution can be expressed as follows:

$$k = \left[k_0^n + \left(k_0 \nu C_k \frac{1}{U_0} \right)^n \right]^{1/n} \tag{24}$$

For the k-relation deduced from the Ergun equation this would read:

$$k = \left[\left(\frac{d_S^2}{150} \frac{\varepsilon^3}{(1-\varepsilon)^2} \right)^n + \left(k_0 \frac{600}{7} \frac{\nu(1-\varepsilon)}{d_S} \frac{1}{U_0} \right)^n \right]^{1/n} \tag{25}$$

One of the authors has used the method suggested by Churchill and Usage (1972) to successfully match asymptotic functions describing the development length of laminar pipe flow. These asymptotic functions for development length were of the same nature as the functions obtained in this paper for the permeability k (see Durst et al. 2005).

The authors of the current paper carried out permeability measurements for porous plates made up of metallic foams with open pores. The presentation of the data showed that $k = f(1/U_0)$ resulted in $\log_{10}$–$\log_{10}$-diagrams that yielded k-variations in the turbulent

flow regime described by straight lines. Using the Ergun equation, this behaviour was also deduced for porous matrices of spherical particles of constant diameter. This finding encouraged the authors to also investigate the permeability of sintered sets of wire meshes. These showed analogous k-distributions, and it is therefore suggested that permeability measurements are presented in the manner proposed in Figs. 8 and 9.

In the literature, see Haas (1982) and Haas and Kulicke (1985), detailed investigation of porous media, made up of spherical particles of nearly equal sizes are described using water as fluid. The results of pressure drop measurements for these porous materials can be presented in the way suggested in this paper. Hence, two parameters k_0 and C_k can be used to characterize this type of porous media and viscous fluids, i.e. also for flows of water. Haas (1982) and Haas and Kulicke (1985) used a method to make up their porous materials yielding the "Ergun constant", to be in the range of 150–180. This is taken into account by different values for the permeabilities k_0.

The results also showed that a dividing line can be deduced from the experimental findings, separating the entire k–$(1/U_0)$ plane into the two regions for laminar and turbulent flows. Permeability measurements should be carried out to yield k_0-values for flows that clearly lie in the laminar flow region. Only in this region is one value of k, namely k_0, measured for all values of $(1/U_0)$ larger than a minimum value.

One interesting topic for future research would be the investigation of the permeability of multiple different porous media in serial arrangement through which a fluid stream flows.

Acknowledgements The authors would like to acknowledge the support of the workshop personnel of FMP Technology in Erlangen, Germany, (in particular Mr. K. Bionenko), for their technical assistance during the measurement process. The work described in this paper received financial support through the NEEDS research project funded by the Federal Ministry for Research and Education (BMBF) in Germany. The project has used the findings of this paper to improve the design of driers for wet-film coated layers with nanoparticles.

Funding Open Access funding enabled and organized by Projekt DEAL.

Data availability The data that support the findings of this study are available from the corresponding author upon reasonable request.

Declarations

Conflict of interest On behalf of all authors, the corresponding author states that there is no conflict of interest.

References

Amazon.com, Inc.: Ölfreie Vakuumpumpe, 220 V, 600 W, ölfreie Kolbenpumpe, 680 mmHg/-90,6 kPa, 160 l/min, Pumpe mit hohem Durchfluss (2020). https://www.amazon.de/%C3%96lfreie-Vakuumpumpe-%C3%B6lfreie-Kolbenpumpe-Durchfluss/dp/B07XQ5KT23. Accessed 10 Feb 2020

Bear, J.: Dynamics of Fluids in Porous Media. American Elsevier, New York (1972)

Bird, R.B., Stewart, W.E., Lightfoot, E.N.: Transport Phenomena. Wiley (1960)

Cambridge AccuSense Inc., Ed.: AIRFLOW-TEMPERATURE MONITOR ATM-24, n.p. (2020). https://www.artisantg.com/info/ATGaygkx.pdf. Accessed 20 Jan 2020

Celik, E., Hoang, L., Ibragimov, A., Kieu, T.: Fluid flows of mixed regimes in porous media. J. Math. Phys. **58**(2), 23102 (2017). https://doi.org/10.1063/1.4976195

Churchill, S.W., Usage, R.: A general expression for the correlation of rates of heat transfer and other phenomenon. AICHE J. **18**, 1121–1132 (1972)

Durst, F., Ray, S., Ünsal, B., Bayoumi, O.A.: The development lengths of laminar pipe and channel flows. J. Fluid Eng. **27**, 1154–1160 (2005)

Durst, F., Ünsal, B.: Forced laminar-to-turbulent transition of pipe flows, J. Fluid Mech. **560**, 449–464 (2006). https://doi.org/10.1017/S0022112006000528

Fourar, M., Radilla, G., Lenormand, R., Moyne, C.: On the non-linear behavior of a laminar single-phase flow through two and three-dimensional porous media. Adv. Water Resour. **27**(6), 669–677 (2004). https://doi.org/10.1016/j.advwatres.2004.02.021

FPZ, Ed.: SIDE CHANNEL BLOWER K 08 TS MOR, n.p. (2015). https://www.fpz.com/datasheet/manuali/DSB_K_08_TS_MOR_IE2_EN_15-05.pdf. Accessed 20 Jan 2020

FR. JACOB SÖHNE GMBH & CO. KG, Ed.: THE CATALOGUE, n.p. (2019). https://www.jacob-pipesystems.com/fileadmin/redakteure/katalog/2019/JACOB_Online-Catalogue-2019_EN-EU_ohnePreise.pdf. Accessed 20 Jan 2020

Freund, H., et al.: Numerical simulations of single phase reacting flows in randomly packed fixed-bed reactors and experimental validation. Chem. Eng. Sci. **58**(3–6), 903–910 (2003). https://doi.org/10.1016/S0009-2509(02)00622-X

Haas, R.: Einfluss von Hochpolymeren auf Sickerströmungen, Dissertation, Universität Karlsruhe, Germany (1982)

Haas, R., Kulicke, W.-M. : Characterisation of dilute polyacrylamide and polystryrene solutions by means of porous media flow. In: Gampert, B. (Ed.) IUTAM Symposium Essen (1984). Springer, Berlin (1985)

Maier, R.S., Kroll, D.M., Bernard, R.S., Howington, S.E., Peters, J.F., Davis, H.T.: Hydrodynamic dispersion in confined packed beds. Phys. Fluids **15**(12), 3795–3815 (2003). https://doi.org/10.1063/1.1624836

MRU GmbH, Ed.: DM 9600 USER MANUAL, n.p. (2018). https://www.mru.eu/fileadmin/user_upload/files/bedienungsanleitungen-en/9122EN_CHP_USER_MANUAL_DM9600.pdf. Accessed 20 Jan 2020

Mucola GmbH: smucola ONLINE SHOPPING: Werkzeuge. http://web.mucola.de/garten_und_terrasse/gartenarbeit/werkzeuge_c112.htm. Accessed 6 Feb 2020.

Wygnanski, I.J., Champagne, F.H.: On transition in a pipe. Part 1. The origin of puffs and slugs and the flow in a turbulent slug, J. Fluid Mech. **59**(2), 281–335 (1973). https://doi.org/10.1017/S0022112073001576

Zeiser, T., Treibig, J., Brenner, G., Durst, F.: Simulation of highly loaded gas-solid two-phase flows by combining a cellular automata for the particles with a lattice Boltzmann flow solver. Int. J. Mod. Phys. B **17**(1–2), 201–204 (2003). https://doi.org/10.1142/S0217979203017333

Zhejiang Wenling Hongbaoshi Vacuum Equipment Factory, Ed.: HBS Wenling Hongbaoshi Vacuum Equipment Factory (2020). http://www.hbspump.com. Accessed 6 Feb 2020